ACS OMEGA

Open Access

This article is licensed under CC-BY-NC-ND 4.0

http://pubs.acs.org/journal/acsodf

Article

Pollutants Analysis and Life Cycle Assessment of a Photovoltaic Powered Textile Electro-Fenton Wastewater Treatment System

Chenyang Zhang, Wei Zhang,* Xiding Zeng, Jiahong Guo, Qing Wang, and Zepu Bai

Cite This: *ACS Omega* 2024, 9, 40477−40484

Read Online

ACCESS | Metrics & More | Article Recommendations | Supporting Information

ABSTRACT: Textile wastewater poses a substantial environmental challenge due to the persistence of organic dyes. This study introduces a novel approach using photovoltaic (PV) powered electro-Fenton (EF) technology for effective treatment of textile wastewater. Acid orange 7 (AO7), methylene blue (MB), and malachite green (MG) were selected as representative organic dyes to validate the method under varying experimental conditions. Analysis of variance (ANOVA) highlighted the significant influence of pollutant type, pH levels, and current density on the degradation efficiency of the system, with optimal conditions observed at pH = 3 and high current density. To underscore the environmental benefits, a comprehensive life cycle assessment (LCA) was conducted. The PV-powered EF system, when implemented in a textile mill, exhibited an energy payback time (EPBT) of 9.53 years, a greenhouse gas payback time (GPBT) of 4.45 years, and a life cycle cost (LCC) of 1.9×10^5 RMB. Comparative analysis with conventional Fenton and EF processes revealed substantial energy savings, with carbon emissions reduced by 95% and 78%, and energy consumption reduced by 87% and 52%, respectively.

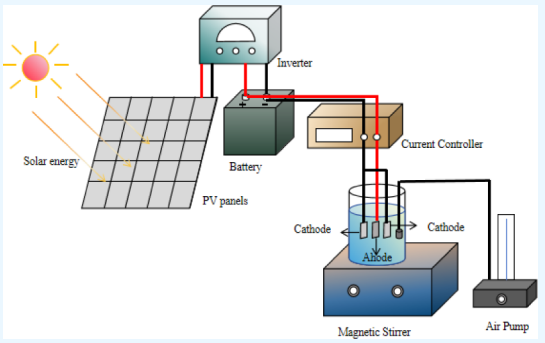

1. INTRODUCTION

Significant environmental pressures are brought about by rapid population growth and urbanization.[1,2] Water pollution, particularly, is considered a critical concern,[3,4] with organic dyes from textile manufacturing posing substantial challenges.[5] These dyes are known to persist in water bodies, disrupting ecological equilibrium,[6,7] and their carcinogenic properties further contribute to environmental and health risks.[8,9] Traditional methods like biological oxidation and chemical flocculation have been found to struggle with effectively addressing these pollutants,[10,11] necessitating advancements in textile wastewater treatment technologies.

The potential of the Fenton reaction has been identified as a solution,[12] where organic dyes are degraded using H_2O_2 and Fe^{2+}.[13] However, challenges in the production and storage of these chemicals have hindered widespread adoption.[14,15] An alternative, the electro-Fenton (EF) process, operates on electrochemical principles, continuously generating Fe^{2+} ions and hydroxyl radicals (HO•) to enhance dye degradation efficiency.[16,17] Despite its effectiveness, the EF process remains reliant on grid electricity, leading to high energy consumption.[18] To address this issue, the integration of renewable energy sources, such as solar energy, is considered crucial. Photovoltaic (PV) panels can be strategically installed in unused spaces such as textile mill roofs and cesspool covers to harness solar power, reducing reliance on conventional grid sources.

Life cycle assessment (LCA) methodology provides a robust framework for evaluating energy consumption and carbon emissions in textile wastewater treatment systems.[19] Estévez et al. performed LCA of technologies for decolorization strategies in textile wastewater to analyze their environmental impacts and economic benefits;[20] Grisales et al. applied LCA to evaluate the impacts of multiple constituents of textile wastewater on the Fenton process;[21] Zhang et al. conducted an LCA of sludge waste reuse in the EF process;[22] Magdy et al. used the LCA approach to compare five methods of chemical removal of phenol and its transformation products containing EF.[23] These studies have applied LCA to assess various aspects of wastewater treatment technologies in the textile sector, highlighting its utility in assessing environmental impacts and economic feasibility.

While existing research has focused on LCA applications in textile wastewater treatment, there remains a gap in evaluating the integration of solar energy to enhance energy efficiency and sustainability. This study aims to fill this gap by implementing a PV-powered EF system and evaluating its performance under

Received: April 9, 2024
Revised: August 30, 2024
Accepted: September 2, 2024
Published: September 17, 2024

ACS Publications

© 2024 The Authors. Published by American Chemical Society

varying operational conditions. An LCA of the system is conducted to compare its environmental and economic benefits against conventional Fenton and EF processes.

The system design and methodology are presented in Section 2. Experimental results are presented in Section 3, followed by the LCA findings in Section 3.2. The main findings of the study are summarized in Section 4.

2. RESEARCH METHOD

2.1. PV-Powered EF System. *2.1.1. Experimental Instruments and Materials.* The PV-powered EF system is primarily composed of a PV system and an EF wastewater treatment system, as depicted in Figure 1's flowchart. The experimental setup can be seen in Figures 2 and 3.

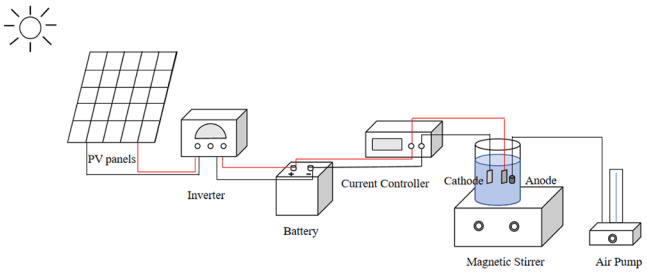

Figure 1. Flowchart of experimental apparatus.

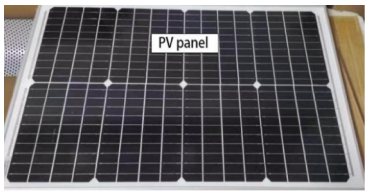

Figure 2. PV panel used in the experiment.

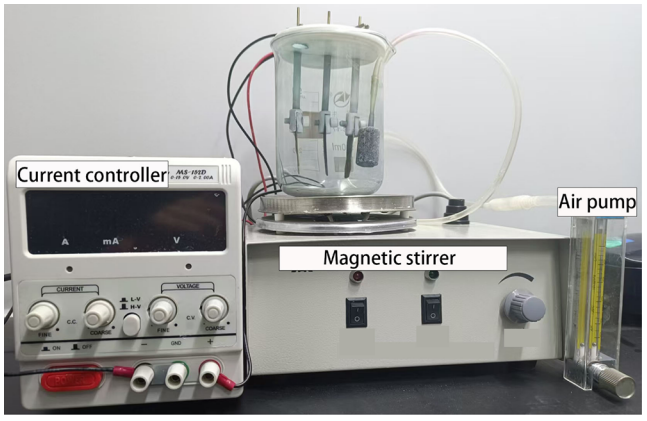

Figure 3. Experimental platform of the EF method.

The PV system includes PV panels connected sequentially to an inverter and then to a battery. Solar energy is absorbed by the PV panels to generate electricity, which is converted from direct current (DC) to alternating current (AC) by the inverter. Any surplus electricity produced is stored in the battery for future use. Situated in Chengdu, China (longitude: 104.00 degrees, latitude: 30.56 degrees north), the experimental platform features PV panels oriented southward at a 30-degree angle from the ground. This orientation optimizes solar energy capture for efficient power generation.

The EF system for wastewater treatment employs nickel foam as the cathode and graphite electrodes as the anode, arranged parallel to the solution. The positive PV pole connects to the anode, while the negative PV pole connects to the cathode, establishing a complete current loop. In the experiment, 400 mL of organic dye wastewater served as the target solution. Continuous oxygenation of the solution was ensured, and degradation rates were monitored by measuring the absorbance using a UV spectrophotometer.

2.1.2. PV System. The Sandia model[24] was used to calculate and evaluate the power production of the PV system. According to calculations performed with this model, the PV system in this experiment is expected to generate 37 kW h annually.

2.1.3. EF Degradation Model. In the experiments, an EF model was used to study the degradation of organic dyes. The process utilizes an electrochemical technique based on the Fenton reaction. The addition of Fe^{2+} acted as a catalyst, initiating the generation of hydroxyl radicals (HO•) crucial for this process, as depicted by eq 1.[25] These hydroxyl radicals possess strong oxidative capabilities, efficiently facilitating the oxidation of organic dyes.

$$Fe^{2+} + O_2{}^* + 2H^+ + 2e^- \rightarrow Fe^{3+} + \bullet OH + OH^- \quad (1)$$

2.2. Analysis of Variance Technique. The statistical analysis of the data was conducted using SPSS software.[26] Multifactor analysis of variance (ANOVA) was employed to determine the statistical significance of differences between data groups, with a significance level set at $p \leq 0.05$. The influence of each factor on the degradation rate was evaluated based on the magnitude of the P-value. Specifically, the analysis concentrated on the individual effects of the three factors, with no consideration of their three-factor interaction.

2.3. Life Cycle Assessment. The LCA method offers a comprehensive approach to evaluate the environmental impact of products, utilizing metrics like energy payback time (EPBT) and greenhouse gas payback time (GPBT).[27] These metrics rely on parameters such as global warming potential (GWP) and primary energy demand (PED) within the LCA framework. The efootprint software, utilizing data primarily sourced from the Ecoinvent database, facilitates online LCA analysis.

2.3.1. Life Cycle Inventory. The system implemented in this experiment is customized for textile mills, with all necessary equipment and materials manufactured in China. The system is designed to operate over a service life of 20 years, encompassing five distinct stages: production, transportation, construction, operation, and waste management. The system's boundary conditions are illustrated in Figure 4. During the production phase, components including PV panels, batteries, inverters, current controllers, and air pumps are manufactured. Transportation primarily involves light diesel trucks for road transport, while construction activities are localized within the textile mill premises. In the operational phase, energy consumption primarily stems from the PV system. Waste generated during the system's lifecycle is typically managed through methods such as adsorption or REDOX processes.

2.3.2. Environmental Impact Assessment. 2.3.2.1. Energy Payback Time. EPBT signifies the duration in years that a PV system requires to generate sufficient energy throughout its lifecycle to offset the energy consumed during its production. The calculation formula for EPBT is expressed in eq 2:

https://doi.org/10.1021/acsomega.4c03397
ACS Omega 2024, 9, 40477−40484

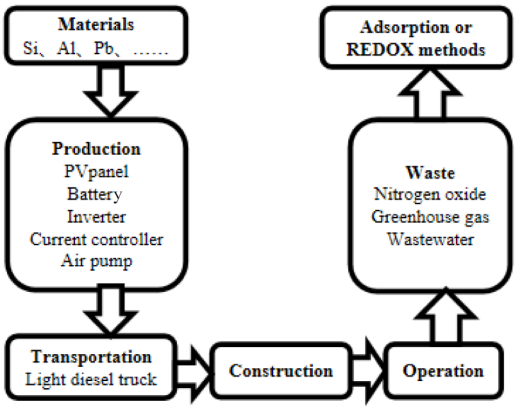

Figure 4. Boundary conditions of the system.

$$\mathrm{EPBT} = \frac{E_{\mathrm{input}} + E_{\mathrm{BOS}}}{E_{\mathrm{output}}} \quad (2)$$

where:

- E_{input} is the primary energy demand (PED) of the PV component during its lifecycle (kW h),
- E_{BOS} is the energy required for the balance of system (BOS) (kW h),
- E_{output} is the annual primary energy saved by the PV system through power generation (kW h).

2.3.2.2. Greenhouse Gas Payback Time. GPBT signifies the duration in years required for a PV system to mitigate carbon emissions over its lifecycle to offset the emissions associated with its production and operation. The calculation formula for GPBT is given by eq 3:

$$\mathrm{GPBT} = \frac{\mathrm{GHG}_{\mathrm{PV}} + \mathrm{GHG}_{\mathrm{BOS}}}{\mathrm{GHG}_{\mathrm{output}}} \quad (3)$$

where:

- $\mathrm{GHG}_{\mathrm{PV}}$ is the global warming potential (GWP) of the PV component during its lifecycle ($\mathrm{kgCO_2eq}$),
- $\mathrm{GHG}_{\mathrm{BOS}}$ is the greenhouse gas emissions from the balance of system (BOS) ($\mathrm{kgCO_2eq}$),
- $\mathrm{GHG}_{\mathrm{output}}$ is the annual primary energy saved by the PV system through power generation ($\mathrm{kgCO_2eq}$).

2.3.3. Life Cycle Cost. Life cycle cost (LCC) serves as a comprehensive metric for evaluating the economic aspects of a system, encompassing all expenses incurred from procurement through to decommissioning. LCC includes costs associated with procurement, transportation, installation, operation, maintenance, management, and decommissioning over the system's lifecycle. The calculation method for LCC considers fixed costs, variable costs, maintenance and operation expenses, salvage value, and other pertinent factors specific to PV panels.[28]

3. RESULTS AND DISCUSSION

3.1. The Experiment on the Degradation of Organic Dyes. The experimental setup in the controlled laboratory conditions was as follows: the temperature was maintained at 16 °C, using a 400 mL sample of pollutant solution with a concentration of 20 mg/L. Oxygen was supplied via an oxygen pump at a rate of 0.6 L/min, and Fe^{2+} was added to maintain a controlled concentration of 200 μmol/L. The absorbance of the solution was measured continuously. Samples were collected every minute following the initiation of current injection to calculate the degradation rate of pollutants.

The study investigated the degradation rates of three different organic dyes—acid orange 7 (AO7), methylene blue (MB), and malachite green (MG)—under varying conditions of organic dye type, current density, and pH. These dyes were chosen due to their diverse colors and chemical structures. The findings contribute to verifying the general applicability of the system for treating organic dye effluents in textile mills. Specifically, the output current was varied by 5 mA, 10 mA, and 15 mA, while pH conditions ranged from 2, 3, to 4.

3.1.1. Effect of the Type of Organic Dye. Various organic dyes are extensively used in textile factories, and their degradation efficiencies vary across different EF systems, which determines the suitability of PV-powered EF systems for treating textile factory wastewater. Therefore, AO7, MB, and MG organic dyes were selected for degradation under controlled conditions: pollutant concentration of 20 mg/L, current density set at 10 mA, and pH maintained at 3. The experimental results are illustrated in Figure 5.

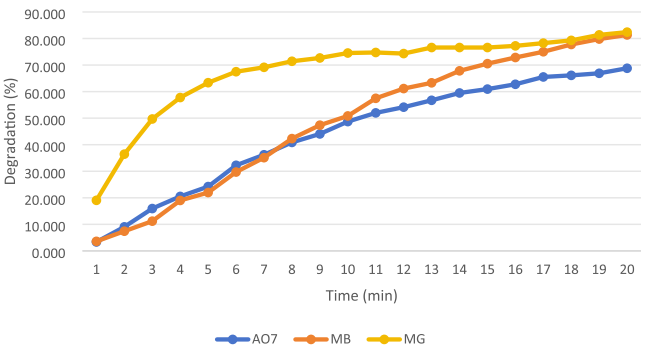

Figure 5. Comparison of degradation rate of three kinds of pollutants.

Effective degradation capabilities for all three pollutants were demonstrated by the system, with degradation rates exceeding 50% within 20 min. The highest degradation efficiency was exhibited by MG, achieving a maximum degradation rate of 82% within 20 min, closely followed by MB at 81%. In contrast, a lower degradation rate of only 69% was shown by AO7. This variation was attributed to the differing numbers of readily oxidizable functional groups in the molecular structures of the pollutants.

In Figure 6, the energy consumption during the degradation of the three pollutants through the EF process is illustrated. It is observed from the comparison that under identical experimental conditions, the energy consumption for AO7 degradation is the highest, followed by MB, while MG shows the lowest energy consumption. This difference is likely associated with the degradation rate, where faster degradation generally corresponds to lower energy consumption.

3.1.2. Effect of pH. The efficiency of EF degradation is notably influenced by pH levels. The degradation rate of AO7 under pH conditions adjusted to 2, 3, and 4 is illustrated in Figure 7. Upon comparison of the degradation rates after 20 min across these pH conditions, it was observed that pH 3 yielded the highest degradation rate, approximately 72%. Furthermore, the degradation of pollutants remained consistently high throughout the experiment under pH 3

https://doi.org/10.1021/acsomega.4c03397
ACS Omega 2024, 9, 40477−40484

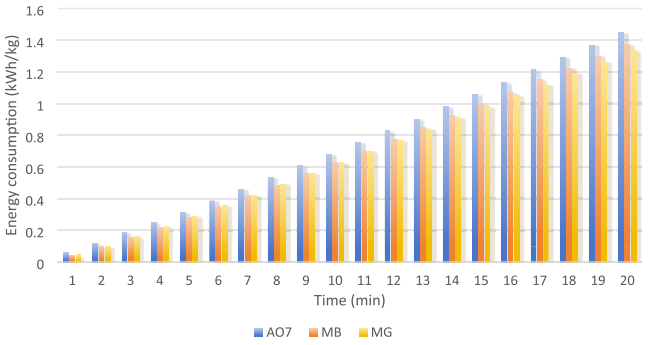

Figure 6. Energy loss in the degradation process of three pollutants.

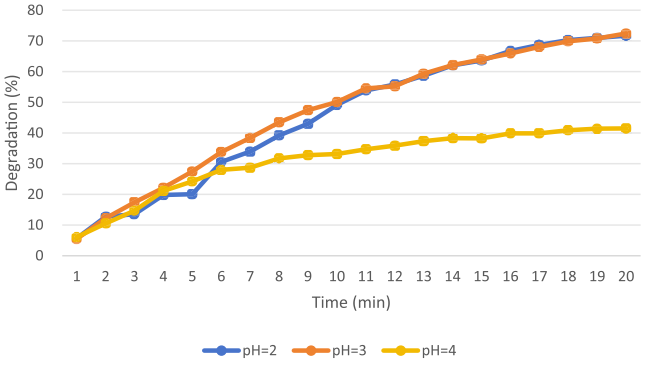

Figure 7. PH affects the degradation rate of AO7.

conditions. Thus, pH around 3 is identified as the optimal condition for EF-mediated removal of target pollutants.

The degradation efficacy can be adversely impacted by a decrease in pH, possibly due to an excess of hydrogen ions. At low pH levels, the stability of H_2O_2 in solution is enhanced by the presence of hydronium ions ($H_3O_2^+$).[29] Simultaneously, hydrogen gas is produced through cathodic reduction, resulting in the reduction of hydroxyl radicals (HO•) production and thereby reducing oxidation efficiency.[30] Conversely, a significant decline in degradation efficiency is brought about by increasing solution pH, likely attributable to the reduced availability of Fe^{2+} ions. As Fe^{2+} is oxidized to Fe^{3+} and precipitates at higher pH levels, the concentration of Fe^{2+} required for catalyzing the Fenton reaction is diminished.[31]

Under the same experimental conditions, MB and MG were selected as pollutants for further investigation, and the results are presented in Figures 8 and 9. The experimental outcomes for MB were found to be consistent with the previously drawn conclusions, confirming their alignment. After a certain duration, stabilization of the degradation rate curve for MG is observed, indicating sustained degradation of the pollutant

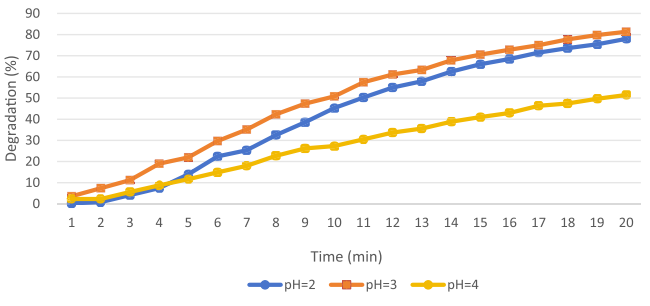

Figure 8. PH affects the degradation rate of MB.

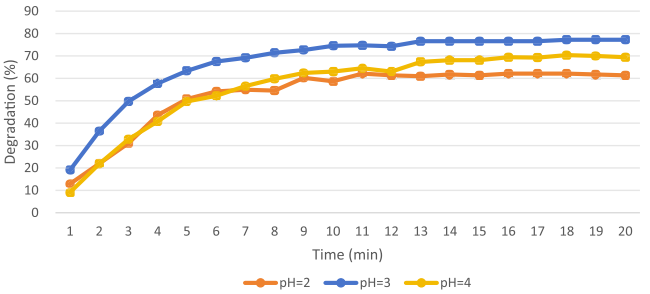

Figure 9. PH affects the degradation rate of MG.

without further rate increase. Specifically, stability is reached in approximately 10 min under pH = 3, around 11 min under pH = 2, and after about 13 min under pH = 4. These findings support the conclusion that stable degradation of pollutants is maintained under optimal pH conditions around 3. The experimental results corroborate the earlier conclusions regarding the effect of pH on pollutant degradation efficiency.

Figure 10 depicts the energy consumption associated with the degradation processes of AO7, MB, and MG by the EF

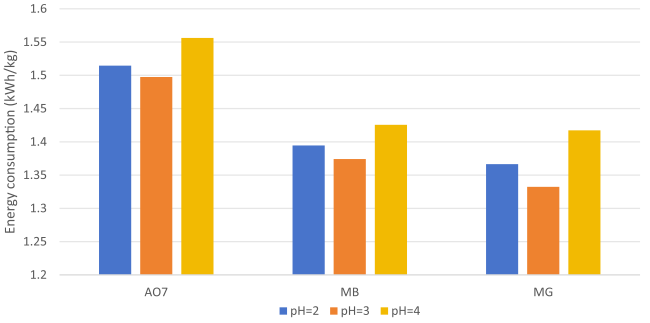

Figure 10. PH affects the energy consumption of the three organic dyes.

system under pH conditions of 2, 3, and 4. It was observed that the lowest energy consumption for all three pollutants was recorded at pH 3. Additionally, considering that the degradation efficiencies of AO7, MB, and MG were highest at pH 3, a correlation between degradation rate and energy consumption is hypothesized. At higher degradation rates, the concentration of dyes in the solution is reduced, leading to a decrease in the consumption of HO• generated during the EF process. The accumulation of HO• is subsequently diminished, reducing their production rate and thereby lowering the overall power consumption of the current loop and energy consumption.

3.1.3. Effect of Current Density. The efficiency of oxygen reduction in the EF system is influenced directly by the applied current. Figure 11 illustrates the degradation rates of acid AO7 under current densities of 5 mA, 10 mA, and 15 mA. After 20 min of treatment, AO7 was degraded to 67% at 5 mA, 68% at 10 mA, and 69% at 15 mA. Furthermore, an increase in the slope of the degradation curve was noted with higher current densities, indicating that the degradation rate was accelerated with increased current. It was observed that AO7 degradation is more effective at higher current densities. This phenomenon is attributed to the higher cathode-imposed potential at increased currents, which enhances the conversion of pumped oxygen to H_2O_2 and increases the production of HO• through

https://doi.org/10.1021/acsomega.4c03397
ACS Omega 2024, 9, 40477−40484

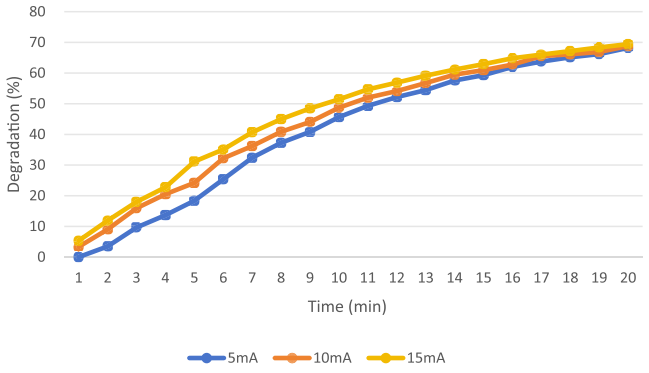

Figure 11. Current density affects the degradation rate of AO7.

electrolysis. The role played by these radicals in accelerating the oxidative degradation of pollutants is crucial.[32]

Figures 12 and 13 illustrate the degradation results of MB and MG under current densities of 5 mA, 10 mA, and 15 mA,

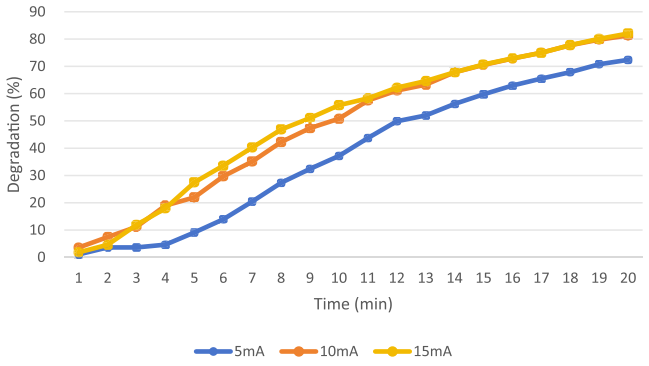

Figure 12. Current density affects the degradation rate of MB.

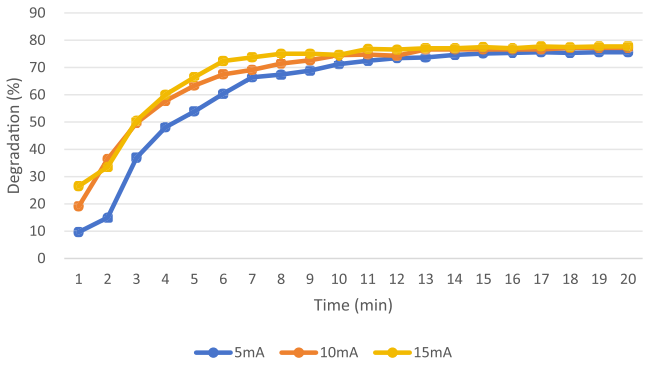

Figure 13. Current density affects the degradation rate of MG.

respectively. For MB, an improvement in degradation efficiency was observed with increasing current density. Specifically, higher degradation rates were achieved at 15 mA compared to 10 mA and 5 mA conditions. Under different current conditions, the degradation rate of MG is stabilized over time: approximately 14 min at 5 mA, 13 min at 10 mA, and only 11 min at 15 mA. A positive correlation between degradation efficiency and higher current densities is confirmed by this observation. The beneficial impact of higher currents in enhancing the effectiveness of both MB and MG degradation in the EF system is underscored by these findings.

Figure 14 depicts the energy loss associated with the degradation processes of AO7, MB, and MG under the current

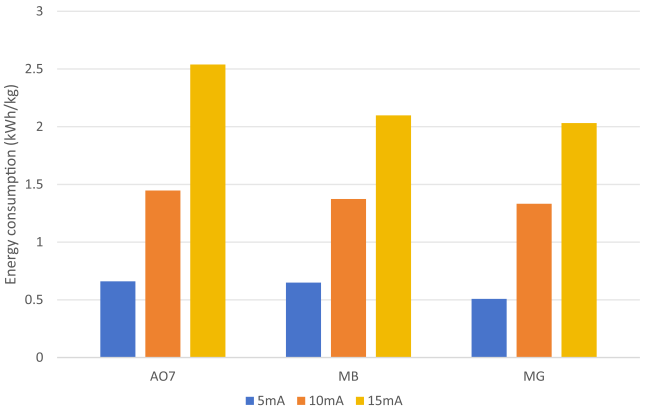

Figure 14. Current density affects the energy consumption of the three organic dyes.

density conditions of 5 mA, 10 mA, and 15 mA. Throughout the EF process system, increased power consumption is caused by higher current densities, which accelerate reaction rates and induce higher potential differences. The generation of more HO• is driven by this heightened potential difference, and an excess of these radicals accumulates in the solution, resulting in additional energy consumption.

3.1.4. Analysis of Variance. The results of multifactor ANOVA were summarized in Table 1 based on the analysis of experimental data. It was found that degradation rates are significantly influenced by the type of organic dyes, pH, and current density. Among the factors analyzed, the most substantial impact on degradation rates was exerted by the type of organic dyes, followed by current density. The effect of pH, however, was observed to be comparatively less significant.

3.2. The Life Cycle Assessment of the PV-Powered EF System. In this section, the LCA of the PV-powered EF system is presented. Initially, the system was applied for wastewater treatment at a textile mill located in Chengdu. The environmental impact of the system was comprehensively analyzed, followed by an evaluation of its cost-effectiveness and economics. Subsequently, comparisons were made between the energy consumption and carbon emissions of the PV-powered EF system and those of conventional Fenton and EF processes to highlight its energy-saving advantages.

3.2.1. The LCA of the System in a Textile Mill. The feasibility of the PV-powered EF system was assessed by selecting a textile mill in Chengdu as the study site. Each day 15,000 m^3 of textile wastewater containing organic dyes is processed at this mill. The existing deep treatment process is replaced by the PV-powered EF system to enhance the degradation of organic dyes during wastewater treatment. A PV capacity of 4.5 MWp has been installed at the textile mill, meeting the energy requirements for operating the system. The electricity generated by the PV system is used to power EF system components such as agitators and air pumps, reducing dependence on the municipal grid.

Figure 15 depicts the GWP and PED of each component in the PV-powered EF system utilized for wastewater treatment at the textile mill. The total PED of the system amounts to 7.61×10^5 MJ, with 3.64×10^5 MJ attributed to PV panels (47.8% of the total). The GWP of the system is 56.24 tCO_2eq, with PV panels contributing 28.37 tCO_2eqs (50.4% of the total). Batteries and inverters also exert significant influence on the environmental assessment of the entire system.

https://doi.org/10.1021/acsomega.4c03397
ACS Omega 2024, 9, 40477−40484

Table 1. ANOVA Results of Degradation Rate

Factor	Degrees of Freedom	Sum of Squares	Mean Square	*F*-Value	*P*-Value	
organic dye types	2	0.029761	0.014880	232.58	<0.0001	significant
pH	2	0.005415	0.002707	8.46	0.0260	significant
current density	2	0.016293	0.008146	24.27	0.0017	significant

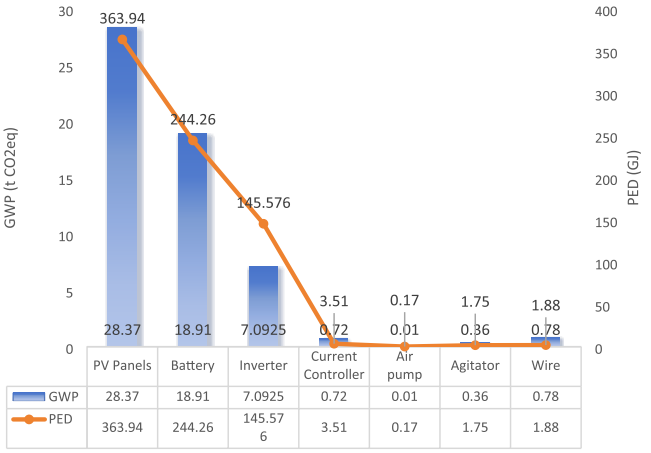

Figure 15. Environmental impact assessment of each component of the system used in a textile mill.

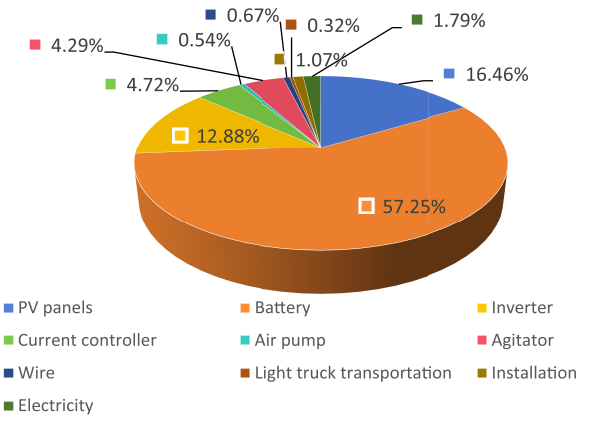

Figure 16. Percentage of cost for each piece of equipment.

3.2.2. Environmental Influence. Eqs 2 and 3 were used to calculate the EPBT and GPBT for the entire PV-powered EF system at the textile mill. Throughout its life cycle, the total PED of the system amounts to 7.61×10^5 MJ, which translates to 2.11×10^5 kW h. The total GWP of the system is computed as 56.24 tCO_2eq. Annually, 22.15 MW h of electricity is generated by the PV power generation system installed at the textile plant, resulting in a reduction of approximately 12.63 tons of CO_2 emissions per year. The system's EPBT is calculated to be 9.53 years, with a GPBT of 4.45 years, both falling within the 20-year system design life, indicating feasible energy recovery and carbon emission reduction over the entire life cycle.

3.2.3. Life Cycle Cost of the System in a Textile Mill. The calculated investment costs for equipping the textile mill with the PV-powered EF system are presented in Table 2. The LCC of the system in the textile mill amounts to 1.9×10^5 RMB. Figure 16 illustrates the cost distribution among various components of the system. The majority of the total expenditure is constituted by the acquisition costs of PV panels, batteries, inverters, and current controllers. Importantly, the overall cost structure is significantly influenced by the high market prices of batteries, inverters, and PV panels. Therefore, to enhance economic efficiency, thorough comparisons should be conducted during equipment procurement. Consideration should be given to selecting batteries, inverters, and PV panels based on their pricing and their ability to meet operational requirements.

Table 2. Cost of Investment in the EF Powered by PV System

Item	Unit Price	Quantity	Total Price (RMB)
PV panels	0.1 yuan/W	260 kW	2.6×10^4
battery	3680 yuan/piece	30 pieces	1.1×10^5
inverter	808 yuan/piece	30 pieces	2.4×10^4
current controller	1900 yuan/piece	4 pieces	7.6×10^3
air pump	14 yuan/piece	40 pieces	5.6×10^2
agitator	3500 yuan/piece	2 pieces	7×10^3
wire	0.94 yuan/m	1000 m	9.4×10^2
light truck transportation	0.1 yuan/(t·km)	1500 t·km	1.5×10^2
installation	57 yuan/m^2	260 m^2	1.5×10^4
electricity	0.63 yuan/kW h	404 kWh	2.5×10^3
sum			1.9×10^5

The annual electricity generation from the PV system applied to the wastewater treatment system of this textile mill amounts to 22.15 MW h. If this electricity had been sourced from the city's grid, it would have incurred a cost of 1.4×10^4 RMB annually. Based on this comparison, the LCC of the PV-powered EF system applied to the textile mill can be recovered within 13.57 years.

It is indicated by this calculation that beyond 13.57 years of service life, the economic benefits of implementing the PV-powered EF system will surpass those of the conventional EF system. The long-term economic viability and financial advantages associated with adopting renewable energy solutions for wastewater treatment in industrial settings are underscored.

3.2.4. Advantages of the System. If the target textile mill were to adopt the Fenton process, annual consumption of H_2O_2 would amount to 26.59 tons. The average production and storage energy consumption per ton of H_2O_2 is 3 MW h, resulting in a carbon footprint of approximately 2 tons. The total energy consumption for this process reaches 79.77 MW h, with a corresponding carbon footprint of 53.18 tons. Alternatively, using the EF process would entail an annual electricity consumption of about 22.15 MW h, leading to emissions equivalent to 12.63 tons of CO_2.

In contrast, if the PV-powered EF system constructed in this study were adopted, the energy consumption for the target textile mill would be reduced to 10.55 MWh. This represents an 87% reduction compared to the Fenton method and a 52% reduction compared to the EF method. In terms of carbon emissions, the system would emit only 2.81 tons of CO_2,

https://doi.org/10.1021/acsomega.4c03397
ACS Omega 2024, 9, 40477−40484

marking a 95% reduction compared to the Fenton method and a 78% reduction compared to the EF method. Figure 17

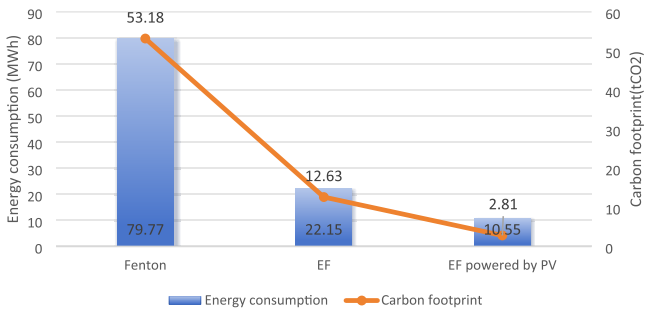

Figure 17. Comparison of energy consumption and carbon footprint of the three systems.

compares the LCA results of the three systems, highlighting the substantial environmental benefits and efficiency gains of the PV-powered EF system over traditional Fenton and EF methods.

The energy consumption of the EF process is primarily influenced by the energy used in the production, installation, and operational electricity requirements of its equipment. In contrast, significantly more energy is required for the production and storage of Fenton reagents in the traditional Fenton process compared to the EF process. As a result, substantial advantages in terms of energy efficiency and reduced carbon emissions are provided by the EF process.

In this paper, the energy supply structure is transformed by integrating PV modules that harness solar energy, a renewable resource, to replace the reliance on the urban grid for powering the EF process. This transition resulted in a reduction in urban grid power consumption, particularly in terms of carbon emissions. Significant CO_2 emissions are typically produced by urban power generation, whereas the clean characteristics of solar energy led to a marked decrease in the carbon footprint of the system compared to both the Fenton and EF processes.

4. CONCLUSION

The development of a PV-powered EF system for the degradation of organic dyes in wastewater treatment is presented in this paper. A significant advancement in achieving energy-efficient solutions for deep wastewater treatment processes is represented by the system. Through LCA, the system's environmental benefits and economic feasibility are evaluated. Several advantages are offered by implementing the PV-powered EF system in textile mills. Reliance on the grid and conventional energy sources is reduced, leading to anticipated savings in energy costs and improvements in overall economic efficiency. By leveraging solar energy, a renewable resource, lower carbon emissions are contributed by the system compared to traditional wastewater treatment methods.

1 A PV-powered EF degradation system for organic dyes was constructed. The system integrates a PV system with an EF system, designed to enhance the deep treatment process of textile mill wastewater and achieve efficient degradation of organic dyes, accompanied by significant economic benefits. Furthermore, the system demonstrates notable energy-saving advantages in terms of reduced energy consumption and carbon emissions.

2 The degradation rate and energy consumption of various organic dyes under different operational conditions were systematically investigated to validate the system's efficacy in textile mill wastewater treatment. Notably, the degradation efficiencies for AO7, MB, and MG reached 82%, 81%, and 69%, respectively, within a 20 min time frame. Optimal experimental conditions were identified at pH = 3 and the highest current density of 15 mA. Additionally, there exists an inverse relationship between energy consumption and degradation rate magnitude. Statistical analysis using ANOVA confirmed significant effects of pollutant type, pH, and current density on the system's degradation rate.

3 This paper conducted an LCA of the PV-powered EF system applied to wastewater treatment in textile mills. The EPBT for the system installed in a Chengdu textile mill was estimated at 9.53 years, with a GPBT of 4.45 years. The LCC was calculated at 1.9×10^5 RMB, ensuring energy recovery over the system's service life. Furthermore, comparing the LCA results with traditional Fenton and EF processes, the PV-powered EF system demonstrated an 87% reduction in energy consumption compared to Fenton and a 52% reduction compared to EF. Carbon emissions were similarly reduced by 95% compared to Fenton and 78% compared to EF, highlighting its substantial energy-saving advantages.

Areas for improvement in this study are still noted, which also point to directions for future research. (1) Three specific organic dyes in the wastewater treatment system of textile mills were focused on, without consideration of potential interactions among various dyes commonly found in actual textile mill effluents. Future research could explore the mixed conditions of different dyes to better reflect real-world scenarios. (2) The LCA conducted in this study relied solely on statistical data, lacking error analysis that could affect result accuracy. Future studies should incorporate error analysis to account for uncertainties and enhance the robustness of LCA findings.

■ ASSOCIATED CONTENT

Supporting Information

The Supporting Information is available free of charge at https://pubs.acs.org/doi/10.1021/acsomega.4c03397.

The life cycle inventory and relevant parameters of the main instruments and materials of the experiment (PDF)

■ AUTHOR INFORMATION

Corresponding Author

Wei Zhang − *College of Architecture and Environment, Sichuan University, Chengdu 610065, China;* orcid.org/0009-0002-4876-8759; Email: zhangwei821@scu.edu.cn

Authors

Chenyang Zhang − *College of Architecture and Environment, Sichuan University, Chengdu 610065, China*

Xiding Zeng − *College of Architecture and Environment, Sichuan University, Chengdu 610065, China*

Jiahong Guo − *College of Architecture and Environment, Sichuan University, Chengdu 610065, China*

Qing Wang − *College of Architecture and Environment, Sichuan University, Chengdu 610065, China*

https://doi.org/10.1021/acsomega.4c03397
ACS Omega 2024, 9, 40477−40484

Zepu Bai − *College of Architecture and Environment, Sichuan University, Chengdu 610065, China*

Complete contact information is available at: https://pubs.acs.org/10.1021/acsomega.4c03397

Notes

The authors declare no competing financial interest.

■ ACKNOWLEDGMENTS

This research has been funded by the Sichuan Science and Technology Program, China (2023YFG0256), the China Construction Eighth Engineering Division (21H1149), and the Sichuan University Creative Research Project (2023SCUH0087).

■ REFERENCES

(1) Zhang, L.; Gu, Q.; Li, C.; Huang, Y. Characteristics and Spatial-Temporal Differences of Urban "Production, Living and Ecological" Environmental Quality in China. *Int. J. Environ. Res. Public Health* **2022**, *19* (22), 15320.

(2) Cao, Y.; Kong, L.; Ouyang, Z. Characteristics and Driving Mechanism of Regional Ecosystem Assets Change in the Process of Rapid Urbanization—A Case Study of the Beijing−Tianjin−Hebei Urban Agglomeration. *Remote Sens. (Basel)* **2022**, *14* (22), 5747.

(3) Wu, J.; Zhang, Q.; Guo, C.; Li, Q.; Hu, Y.; Jiang, X.; Zhao, Y.; Wang, J.; Zhao, Q. Effects of Aeration on Pollution Load and Greenhouse Gas Emissions from Agricultural Drainage Ditches. *Water (Basel)* **2022**, *14* (22), 3783.

(4) Moiseenko, T. I. Surface Water under Growing Anthropogenic Loads: From Global Perspectives to Regional Implications. *Water (Basel)* **2022**, *14* (22), 3730.

(5) Zhang, W.; Liu, Y.; Du, L. Sol-Gel Preparation of Photocatalytic Sm2Ti2O7/HZSM-5 Composite on Degradation of Reactive Brilliant Red X-3B. *Mater. Sci.* **2018**, *24* (3), 307−311.

(6) Abdelhameed, R. M.; Emam, H. E. Modulation of metal organic framework hybrid cotton for efficient sweeping of dyes and pesticides from wastewater. *Sustainable Mater. Technol.* **2022**, *31*, No. e00366.

(7) Roa, K.; Oyarce, E.; Boulett, A.; ALSamman, M.; Oyarzún, D.; Pizarro, G. D. C.; Sánchez, J. Lignocellulose-Based Materials and Their Application in the Removal of Dyes from Water: A Review. *Sustainable Mater. Technol.* **2021**, *29*, No. e00320.

(8) de Oliveira Cruz, F. S.; Nascimento, M. A.; Puiatti, G. A.; de Oliveira, A. F.; Mounteer, A. H.; Lopes, R. P. Textile Effluent Treatment Using a Fixed Bed Reactor Using Bimetallic Fe/Ni Nanoparticles Supported on Chitosan Spheres. *J. Environ. Chem. Eng.* **2020**, *8* (5), 104133.

(9) Salimi, M.; Salar Balou, S.; Kohansal, K.; Babaei, K.; Tavasoli, A.; Andache, M. Optimizing the Preparation of Meso- and Microporous Canola Stalk-Derived Hydrothermal Carbon via Response Surface Methodology for Methylene Blue Removal. *Energy Fuels* **2017**, *31* (11), 12327−12338.

(10) Kumar, P.; Prasad, B.; Mishra, I. M.; Chand, S. Treatment of Composite Wastewater of a Cotton Textile Mill by Thermolysis and Coagulation. *J. Hazard. Mater.* **2008**, *151* (2−3), 770−779.

(11) Can, O. T.; Kobya, M.; Demirbas, E.; Bayramoglu, M. Treatment of the Textile Wastewater by Combined Electro-coagulation. *Chemosphere* **2006**, *62* (2), 181−187.

(12) Wan, W.; Zhang, Y.; Ji, R.; Wang, B.; He, F. Metal Foam-Based Fenton-like Process by Aeration. *ACS Omega* **2017**, *2* (9), 6104−6111.

(13) Divyapriya, G.; Nidheesh, P. V. Importance of Graphene in the Electro-Fenton Process. *ACS Omega* **2020**, *5* (10), 4725−4732.

(14) Elias, B.; Guihard, L.; Nicolas, S.; Fourcade, F.; Amrane, A. Effect of Electro-Fenton Application on Azo Dyes Biodegradability. *Environ. Prog. Sustainable Energy* **2011**, *30* (2), 160−167.

(15) Zhang, S.; Pang, X.; Yue, Z.; Zhou, Y.; Duan, H.; Shen, W.; Li, J.; Liu, Y.; Cheng, Q. Sulfonamides Removed from Simulated Livestock and Poultry Breeding Wastewater Using an In-Situ Electro-Fenton Process Powered by Photovoltaic Energy. *Chem. Eng. J.* **2020**, *397*, 125466.

(16) Berl, E. A New Cathodic Process for the Production of H_2O_2. *Trans. Electrochem. Soc.* **1939**, *76* (1), 359.

(17) Berhe, R. N.; Kassahun, S. K.; Kang, J. W.; Lee, I.; Verma, M.; Kim, H. Performance Evaluation of Fe3O4@ACF-Supported Bio-Electro Fenton System for Simultaneous Sewage Treatment and Methyl Orange Degradation. *Mater. Today Commun.* **2023**, *35*, 106331.

(18) Gao, G.; Zhang, Q.; Hao, Z.; Vecitis, C. D. Carbon Nanotube Membrane Stack for Flow-through Sequential Regenerative Electro-Fenton. *Environ. Sci. Technol.* **2015**, *49* (4), 2375−2383.

(19) Shen, W.; Tian, Z.; Zhao, L.; Qian, F. Life Cycle Assessment and Multiobjective Optimization for Steam Cracking Process in Ethylene Plant. *ACS Omega* **2022**, *7* (18), 15507−15517.

(20) Estévez, S.; Angelucci, D. M.; Moreira, M. T.; Tomei, M. C. Techno-Environmental and Economic Assessment of Color Removal Strategies from Textile Wastewater. *Sci. Total Environ.* **2024**, *913*, 169721.

(21) Grisales, C. M.; Salazar, L. M.; Garcia, D. P. Treatment of Synthetic Dye Baths by Fenton Processes: Evaluation of Their Environmental Footprint through Life Cycle Assessment. *Environ. Sci. Pollut. Res. Int.* **2018**, *26*, 4300−4311.

(22) Zhang, D.; Hu, S.; Cao, Z.; Cao, H.; Zhao, Y.; Zhao, H. Reuse of Sludge Waste in Electro-Fenton: Performance and Life Cycle Assessment. *Resour., Conserv. Recycl.* **2022**, *185*, 106475.

(23) Magdy, M.; Alalm, M. G.; El-Etriby, H. K. Comparative Life Cycle Assessment of Five Chemical Methods for Removal of Phenol and Its Transformation Products. *J. Cleaner Prod.* **2021**, *291*, 125923.

(24) King, D. L.; Boyson, W. E.; Kratochvil, J. A. *Photovoltaic Array Performance Model*; Sandia National Laboratories, 2004.

(25) Wang, X.; Xu, C.; Zhu, Y.; Zhou, C.; Yang, Y.; Miao, J.; Zhou, W.; Shao, Z. The Recent Progress of Cathode Materials for Heterogeneous Electro-Fenton Reactions. *Surf. Interfaces* **2024**, *44*, 103820.

(26) Rasweefali, M. K.; Sabu, S.; Sunooj, K. V.; Sasidharan, A.; Xavier, K. A. M. Consequences of Chemical Deacetylation on Physicochemical, Structural and Functional Characteristics of Chitosan Extracted from Deep-Sea Mud Shrimp. *Carbohydr. Polym. Technol. Appl.* **2021**, *2*, 100032.

(27) Peng, J.; Lu, L.; Yang, H. Review on Life Cycle Assessment of Energy Payback and Greenhouse Gas Emission of Solar Photovoltaic Systems. *Renewable Sustainable Energy Rev.* **2013**, *19*, 255−274.

(28) Singh, D.; Singh, S.; Yadav, A. K.; Khan, O.; Dewangan, A.; Alkahtani, M. Q.; Islam, S. From Theory to Practice: A Sustainable Solution to Water Scarcity by Using a Hybrid Solar Distiller with a Heat Exchanger and Aluminum Oxide Nanoparticles. *ACS Omega* **2023**, *8* (37), 33543−33553.

(29) Zhou, M.; Yu, Q.; Lei, L.; Barton, G. Electro-Fenton Method for the Removal of Methyl Red in an Efficient Electrochemical System. *Sep. Purif. Technol.* **2007**, *57* (2), 380−387.

(30) Ting, W.-P.; Lu, M.-C.; Huang, Y.-H. Kinetics of 2,6-Dimethylaniline Degradation by Electro-Fenton Process. *J. Hazard. Mater.* **2009**, *161* (2−3), 1484−1490.

(31) Solozhenko, E. G.; Soboleva, N. M.; Goncharuk, V. Decolorization of Azo Dye Solutions by Fenton Oxidation. *Water Res.* **1995**, *29* (9), 2206−2210.

(32) Luo, H.; Li, C.; Wu, C.; Dong, X. In Situ Electrosynthesis of Hydrogen Peroxide with an Improved Gas Diffusion Cathode by Rolling Carbon Black and PTFE. *RSC Adv.* **2015**, *5* (80), 65227−65235.